SECTION III. TASK 3. COMPREHENSIVE MODEL DEVELOPMENT AND EVALUATION

Objectives

The objective of this task is to integrate advanced chemistry and physics submodels into a comprehensive two-dimensional model of entrained-flow reactors (PCGC-2) and to evaluate the model by comparing with data from well-documented experiments. Approaches for the comprehensive modeling of fixed-bed reactors will also be reviewed and evaluated and an initial framework for a comprehensive fixed-bed code will be employed after submission of a detailed test plan (Subtask 3.b).

Task Outline

This task will be performed in three subtasks. The first covering the full 60 months of the program will be devoted to the development of the entrained-bed code. The second subtask for fixed-bed reactors will be divided into two parts. The first part of 12 months will be devoted to reviewing the state-of-the-art in fixed-bed reactors. This will lead to the development of the research plan for fixed-bed reactors. After approval of the research plan, the code development would occupy the remaining 45 months of the program. The third subtask to generalize the entrained-bed code to fuels other than dry pulverized coal would be performed during the last 24 months of the program.

III.A. SUBTASK 3.a. -- INTEGRATION OF ADVANCED SUBMODELS INTO ENTRAINED-FLOW CODE, WITH EVALUATION AND DOCUMENTATION

Senior Investigators -- B. Scott Brewster and L. Douglas Smoot

Brigham Young University
Provo, UT 84602
(801) 378-6240 and (801) 378-4326

Objectives

The objectives of this subtask are 1) to improve an existing 2-dimensional code for entrained coal combustion/gasification to be more generally applicable to a variety of coals by incorporating advanced coal chemistry submodels, advanced numerical methods, and an advanced pollutant submodel for both sulfur and nitrogen species, and 2) to validate the advanced submodels in the comprehensive code. The comprehensive code into which the advanced submodels will be incorporated is PCGC-2 (Pulverized Coal Gasification and Combustion 2-dimensional).

Accomplishments

Work on this subtask is being accomplished under five components: 1) the evaluation and incorporation of coal reaction submodels into the comprehensive code, 2) the incorporation of improved numerical solution methods, 3) the incorporation of the SO_x-NO_x submodel developed under Subtask 2.g, 4) implementation of the code on computers, and 5) code evaluation. First-year progress is described below for each of these components.

Component 1 -- Evaluation and Incorporation of Coal Reaction Submodels

This component of the subtask is aimed at selecting coal reaction submodels and developing methodology for incorporating them into PCGC-2. First-year efforts were devoted mainly to devolatilization and the method of integrating the coal-to-char chemistry submodel being developed under Subtask 2.a. Three alternatives are being considered. The first is direct integration of the Functional Group (FG) devolatilization model into the comprehensive code, without modification of the treatment of turbulence-chemistry interaction. This approach is referred to as the Single

Solids Progress Variable (SSPV) Method. The second approach is to extend the current treatment of turbulence-chemistry interaction to specifically account for variability in coal offgas composition. This method is called the Multiple Solids Progress Variable (MSPV) Method. The third approach is to treat the gas phase turbulence in a Lagrangian reference frame with a statistical dispersion model. This approach is referred to as the Statistical Gas Dispersion (SGD) Method. Progress during the first year on each of these three methods is outlined below. In addition, code sensitivity to several thermal parameters affecting devolatilization was investigated, and a model for variable heat capacity was incorporated. Technical presentations were made at the First Annual Technical Review Meeting of the BYU Advanced Combustion Engineering Research Center (ACERC), the Seventh Annual Gasification and Gas Stream Cleanup Systems Contractors Review Meeting sponsored by METC, and at the 194th National Meeting of the American Chemical Society.

Single Solids Progress Variable (SSPV) Method -- The basic assumption of the SSPV Method is that the coal offgas composition is constant. This approach is currently implemented in PCGC-2. Hence, integration of the FG Model under this method is straight-forward. Since offgas composition is assumed constant, only a single progress variable (mixture fraction) is needed to calculate the contribution of solids reaction to the local gas elemental composition. Turbulence/chemistry interaction is accounted for by integrating local instantaneous gas properties calculated from equilibrium over the probability density functions of the coal and inlet gas mixture fractions. The current code also assumes the coal offgas enthalpy is constant, but this can be varied if the energy equation is solved.

The FG Model consists of 19 independent reactions that form gas and one dependent reaction that forms tar. In addition, all 20 reactions have distributed activation energy. The current devolatilization submodel in PCGC-2 cannot accommodate the FG model because it allows only dependent reactions with non-distributed activation energy. Recently, Baxter (1987) implemented a general devolatilization submodel in PCGC-2 that accommodates any number of dependent and independent reactions, all with distributed activation energy. During the next quarter, the FG Model will be tested in

PCGC-2 using this general submodel and the results compared with the 2-equation model used previously.

Multiple Solids Progress Variable (MSPV) Method -- This method allows the coal offgas composition and enthalpy to vary. Coal offgas is known to be richer in hydrogen near the beginning of devolatilization and richer in carbon near the end and throughout the period of char oxidation, after devolatilization is essentially complete. In addition, volatiles emitted near the end of devolatilization are more energetic than early volatiles. Therefore, it is thought that allowing for variable coal offgas composition could have a significant impact on the code predictions. Prediction of minor species, such as pollutants, in gasification processes could be the most significantly affected. The formation of NO, for example, is known to depend on the local equivalence ratio in the region where the nitrogen is emitted from the coal. If nitrogen is emitted in the presence of oxygen, NO is formed. Since a gasifier has both fuel-lean and fuel-rich regions, the location of nitrogen evolution is critical to the prediction of NO formation, and nitrogen is generally known to evolve more slowly than the bulk volatiles.

In the MSPV method, the coal offgas is divided into a number of components, each with constant composition and enthalpy. A separate progress variable is used to track each component, and the interaction of chemistry and turbulence is accounted for as before. The instantaneous properties of the gas are integrated over the joint probability density function of all the mixture fractions to calculate the time-mean properties.

Generalized Theory -- The general theory for the MSPV Method was developed from the theory for two variables as follows. The general definition of N mixture fractions is given by

$$f_1 = \frac{m_1}{m_0 + m_1}$$

$$f_2 = \frac{m_2}{m_0 + m_1 + m_2}$$

$$\vdots$$

$$f_N = \frac{m_N}{m_0 + m_1 + m_2 + \ldots + m_N} = \frac{m_N}{\sum_{i=0}^{N} m_i} \qquad \text{(III.A-1)}$$

Each additional mixture fraction is defined as the mass fraction of an additional component of prescribed composition in the mixture, and all of the previous mixture fractions are defined in terms of a mixture where this component is absent. With this definition, each of the mixture fractions can independently assume values between zero and unity. The subscript "0" will typically refer to the primary stream, "1" will typically refer to the secondary, "2" will typically refer to the first coal offgas component, "3" to the second, and so on. Alternatively, "2" could refer to an additional inlet stream, "3" to another additional inlet, and so forth. Any combination of additional gas inlets and coal offgas components is also possible.

With N independent (in a mathematical sense) mixture fractions, there will be 2N intermittencies to take into account. For each mixture fraction i, there will be the intermittency α_i of the "pure i" gas and $\alpha_{i'}$ of the "i-free" gas. These intermittencies are given by

$$\alpha_i = \frac{1}{\sqrt{2\pi G_{ii}}} \int_{\frac{1-F_i}{\sqrt{G_{ii}}}}^{\infty} \exp\left[\frac{-(f_i - F_i)}{2G_{ii}}\right] df_i \qquad \text{(III.A-2)}$$

$$\alpha_{i'} = \frac{1}{\sqrt{2\pi G_{ii}}} \int_{-\infty}^{\frac{-F_i}{\sqrt{G_{ii}}}} \exp\left[\frac{-(f_i - F_i)}{2G_{ii}}\right] df_i \qquad \text{(III.A-3)}$$

where F_i and G_{fi} are given by the following two coupled equations:

$$\tilde{f}_i = \alpha_i + \frac{1}{\sqrt{2\pi G_{ii}}} \int_0^1 f_i \exp\left[\frac{-(f_i - F_i)}{2G_{ii}}\right] df_i \qquad \text{(III.A-4)}$$

$$\tilde{g}_{ii} = \alpha_i - \tilde{f}_i^2 + \frac{1}{\sqrt{2\pi G_{ii}}} \int_0^1 f_i^2 \exp\left[\frac{-(f_i - F_i)}{2G_{ii}}\right] df_i \qquad \text{(III.A-5)}$$

The time-mean values of dependent fluctuating gas properties are calculated by convolving the instantaneous values over the joint probability

density function of the independent mixture fractions. For an arbitrary number of mixture fractions,

$$\beta(f_N, f_{N-1}, \cdots, f_2, f_1) = \int\int\cdots\int P(f_N, f_{N-1}, \cdots, f_2, f_1) \cdot \beta(f_N, f_{N-1}, \cdots, f_2, f_1) d f_1 \, d f_2 \cdots d f_{N-1} \, d f_N \quad \text{(III.A-6)}$$

At the present time, the theory in the comprehensive code assumes the joint probability density is separable, i.e. for an arbitrary number of mixture fractions,

$$P(f_N, f_{N-1}, \cdots, f_2, f_1) = \prod_{I=1}^{N} P(f_I) \quad \text{(III.A-7)}$$

Equation (6) includes a term accounting for the contribution of each possible combination of fluid components, allowing for each component to be intermittent. The total number of required terms is $4 \cdot 2^N - 1$. The necessary terms for three mixture fractions are tabulated in Table III.A-1. In this case, 15 terms are required ($4 \cdot 2^2 - 1$). With three mixture fractions, mixtures of four fluid components can be described. These are referenced by subscripts 0, 1, 2, and 3. The first term gives the contribution of pure fluid 3. In this case, f_3 is equal to unity. Since fluids 0, 1, and 2 are intermittent, f_1 and f_2 are undefined for this term. The contribution due to pure fluid 3 is therefore equal to the fraction of the total time that the fluid is pure 3 multiplied by the property β of pure 3.

The second term gives the contribution of pure fluid 2. In this case, fluids 0, 1, and 3 are intermittent. Since fluid 3 is intermittent, f_3 is equal to 0. Since 0 and 1 are intermittent, f_2 is equal to 1 and f_1 is undefined. The contribution of pure fluid 2 is given by the the product of α_3', the fraction of time that fluid 3 is totally absent, multiplied by α_2, the fraction of time the fluid is pure component 2, multiplied by the value of β for pure component 2. The third and fourth terms similarly give the contributions of pure fluids 1 and 0.

TABLE III.A-1

CONVOLUTION OF β OVER A SEPARABLE TRIPLE-PROBABILITY DENSITY FUNCTION

No.	f_3	f_2	f_1	Term	Description
1	1	-	-	$\alpha_3 \beta_3$	Pure fluid 3 (intermittency of 0,1, and 2)
2	0	1	-	$\alpha_3.\alpha_2 \beta_2$	Pure fluid 2 (intermittency of 0, 1, and 3)
3	0	0	1	$\alpha_3.\alpha_2.\alpha_1 \beta_1$	Pure fluid 1 (intermittency of 0, 2, and 3)
4	0	0	0	$\alpha_3.\alpha_2.\alpha_1 \beta_1$	Pure fluid 0 (intermittency of 1, 2, and 3)
5	0	0	f_1	$\alpha_3.\alpha_2. \int_{0+}^{1-} P(f_1)\beta(0, 0, f_1)\mathrm{d}f_1$	Mixture of fluids 0 and 1 (intermittency of 2 and 3)
6	0	f_2	1	$\alpha_3.\alpha_1 \int_{0+}^{1-} P(f_2)\beta(0, f_2, 1)\mathrm{d}f_2$	Mixture of fluids 1 and 2 (intermittency of 0 and 3)
7	0	f_2	0	$\alpha_3.\alpha_1. \int_{0+}^{1-} P(f_2)\beta(0, f_2, 0)\mathrm{d}f_2$	Mixture of fluids 0 and 2 (intermittency of 1 and 3)
8	0	f_2	f_1	$\alpha_3. \int_{0+}^{1-} P(f_2) \int_{0+}^{1-} P(f_1)\beta(0, f_2, f_1)\mathrm{d}f_1\mathrm{d}f_2$	Mixture of fluids 0, 1, and 2 (intermittency of 3)

TABLE III.A-1 (cont'd)

CONVOLUTION OF β OVER A SEPARABLE TRIPLE-PROBABILITY DENSITY FUNCTION

No.	f_3	f_2	f_1	Term	Description
9	f_3	1	-	$\alpha_2 \int_{0+}^{1-} P(f_3)\,\beta(f_3, 1)\,d f_3$	Mixture of fluids 2 and 3 (intermittency of 0 and 1); note that β is not a function of f_1
10	f_3	0	1	$\alpha_2\alpha_1 \int_{0+}^{1-} P(f_3)\,\beta(f_3, 0, 1)\,d f_3$	Mixture of fluids 1 and 3 (intermittency of 0 and 2)
11	f_3	0	0	$\alpha_2\alpha_1 \int_{0+}^{1-} P(f_3)\,\beta(f_3, 0, 0)\,d f_3$	Mixture of fluids 0 and 3 (intermittency of 1 and 2)
12	f_3	0	f_1	$\alpha_2 \int_{0+}^{1-} P(f_3) \int_{0+}^{1-} P(f_1)\,\beta(f_3, 0, f_1)\,d f_1\,d f_3$	Mixture of fluids 0,1, and 3 (intermittency of 2)
13	f_3	f_2	1	$\alpha_1 \int_{0+}^{1-} P(f_3) \int_{0+}^{1-} P(f_2)\,\beta(f_3, f_2, 1)\,d f_2\,d f_3$	Mixture of fluids 1, 2, and 3 (intermittency of 0)
14	f_3	f_2	0	$\alpha_1 \int_{0+}^{1-} P(f_3) \int_{0+}^{1-} P(f_2)\,\beta(f_3, f_2, 0)\,d f_2\,d f_3$	Mixture of fluids 0, 2, and 3 (intermittency of 1)
15	f_3	f_2	f_1	$\int_{0+}^{1-} P(f_3) \int_{0+}^{1-} P(f_2) \int_{0+}^{1-} P(f_1)\,\beta(f_3, f_2, f_1)\,d f_1\,d f_2\,d f_3$	Mixture of fluids 0, 1, 2, and 3 (no intermittency)

The fifth through fifteenth terms give the contributions of various mixtures of the four fluids. Where mixture fractions can take on values between 0 and 1, and the respective fluids are not intermittent, this is indicated by an f_1, f_2, etc., in the appropriate column. The property β must then be integrated over the probability density functions of the variable mixture fractions to calculate the contribution of that particular mixture. The fifteenth term gives the contribution of a mixture where there is no intermittency, i.e. when all mixture fractions are continuously variable over the range 0 to 1.

The pattern for extending Table III.A-1 to N mixture fractions is straight-forward. First, a fluid intermittency matrix consisting of N columns and $4 \cdot 2^N - 1$ rows should should be constructed. The columns should be ordered from highest to lowest, as in Table III.A-1. The first N rows in the matrix will correspond to pure fluids 1 through N. These are indicated by a "1" in column for the appropriate mixture fraction and a "0" for all higher order mixture fractions. Lower order mixture fractions are not meaningful in this case, since there none of the lower order fluids are present. The $N+1^{st}$ row will correspond to pure fluid 0. This is indicated with a "0" in all N columns. The remaining rows correspond to mixtures where at least one fluid is non-intermittent. The final row corresponds to the mixture where all N+1 fluids are non-intermittent. Of course, this order of rows and columns is arbitrary and is only suggested as a convenient procedure for writing down all the necessary terms.

Each term will contain a contribution from each of the meaningful mixture fractions multiplied by the property β evaluated at the proper values of the mixture fractions. The contribution for each mixture fraction with a value of unity is α_i. The contribution for each mixture fraction with a value of zero is $\alpha_{i'}$. The contribution for each mixture fraction that is continuously variable is the integral over the probability density function. Of course, if any of the meaningful mixture fractions are variable, β must be placed inside the integral(s).

The MSPV Method does not allow the coal offgas composition and enthalpy to vary continuously unless the number of progress variables is equal to the

number of chemical species or elements being evolved at similar rates from the coal. However, the approach is being tested in a limited fashion using the two existing progress variables in PCGC-2 (f and η) to both track coal offgas. This investigation is described below.

Two Progress Variables to Track Coal Offgas -- In joint consultation with AFR, it was decided that the best initial approach at dividing the offgas between two progress variables is to divide the offgas into products of devolatilization and products of char oxidation. The oxidation offgas can be assumed to be pure carbon (other elements in the actual chemicals originate from the inlet gas), and the elemental composition of the devolatilization products can be calculated by material balance, assuming a value for ultimate volatiles yield, e.g. 40 percent. The mixture fraction f can be used to track the char oxidation offgas (i.e. residual carbon after oxidation) and η can be used to track the volatile products. Therefore, f and η would be redefined as follows for the purposes of this calculation:

$$f = \frac{\dot{m}_h}{\dot{m}_p + \dot{m}_s + \dot{m}_v} \qquad \text{(III.A-8)}$$

$$\eta = \frac{\dot{m}_v}{\dot{m}_p + \dot{m}_s + \dot{m}_c} \qquad \text{(III.A-9)}$$

where $\dot{m}_h$ is the mass flowrate of char oxidation offgas (pure carbon), $\dot{m}_v$ is the the mass flowrate of volatiles offgas, $\dot{m}_p$ is the mass flowrate of primary gas, $\dot{m}_s$ is the mass flowrate of secondary gas, and $\dot{m}_c$ is the total offgas flowrate, given by

$$\dot{m}_c = \dot{m}_v + \dot{m}_h \qquad \text{(III.A-10)}$$

The mixture fraction η therefore represents the local mass fraction of volatiles and f represents the local mass fraction of carbon in the volatiles-free gas that originated from the coal.

Code modifications have been carried out according to the above definitions, and calculations are being performed for a trial case where the

primary and secondary gas inlet streams have identical compositions. Depending on the results of this investigation, it is anticipated that additional progress variables for coal offgas may soon be added, since more than two progress variables are likely needed for the coal, and f is normally needed to track the mixing of inlet gas streams. However, it is recognized that the total number of mixture fractions used in any given simulation should be kept to a minimum due to the complications of turbulence/chemistry interactions, as described below.

Effects of Turbulence/Chemistry Interactions -- The extension of the code to multiple progress variables under the MSPV Method described above is significantly complicated by the interaction of chemistry and turbulence. This interaction arises due to the nonlinear dependence of chemical kinetics on temperature and reactant concentrations. It is ignored for heterogeneous reactions because the time scales of these reactions are long compared to the time scale of the turbulence. However, the time scales of the homogeneous reactions of the volatiles in the gas are much shorter. PCGC-2 assumes local instantaneous equilibrium for the gas and calculates time-mean properties by convolving the instantaneous values over the probability density functions of the mixture fractions. If the effects of the turbulent fluctuations on the time-mean properties of the gas phase could be neglected, additional mixture fraction variables would not significantly increase the required computer time, because this convolution would be unnecessary.

Although the effect of neglecting turbulent fluctuations on comprehensive code predictions has been clearly demonstrated (Smith and Fletcher, 1986), additional calculations were performed to investigate the sensitivity of individually neglecting fluctuations in the inlet gas mixture fraction f and the coal gas mixture fraction η. In the first set of calculations, a fuel-lean (combustion) case was investigated. The primary and secondary gas streams were identical in composition (both were air) and differed only in temperature (the secondary was preheated). It was observed in this case that turbulent fluctuations are important and need to be taken into account for but not for f, as illustrated in Figure III.A-1. For centerline gas temperature and radially integrated burnout, the values for the base case (fluctuations in both f and η) and Case 3 (ignore fluctuations in f) were

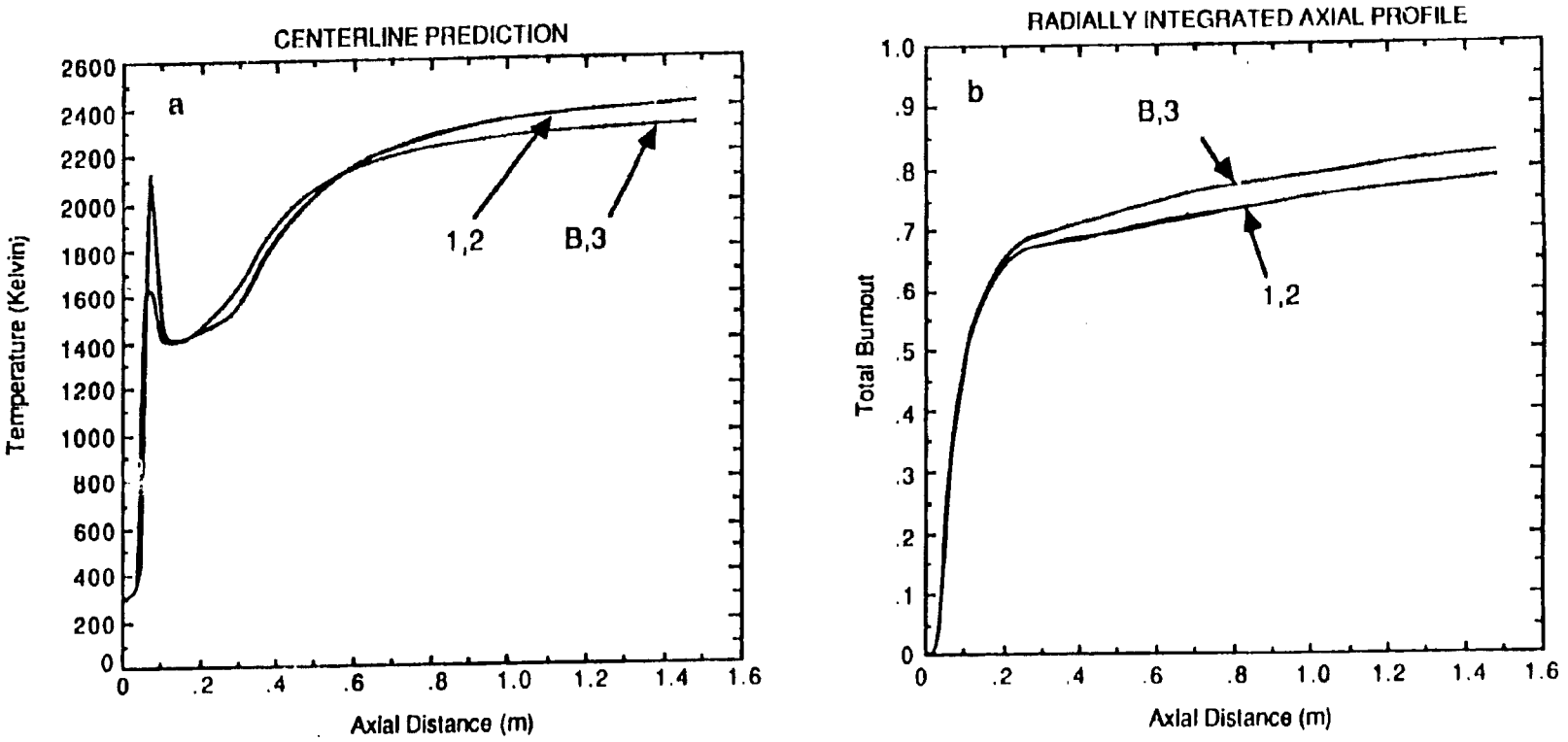

Figure III.A-1. Effect of ignoring turbulent fluctuations of inlet gas and coal gas mixture fractions on predictions for pulverized coal combustion.

B-Base case
1-Ignore η fluctuations
2-Ignore f and η fluctuations
3-Ignore f fluctuations

nearly identical. The values for Case 1 (ignore η fluctuations) and Case 2 (ignore both f and η fluctuations) were also nearly identical, but differed significantly from the other two cases. Therefore, for a case where the primary and secondary streams differed in temperature but not in composition, the fluctuations in coal gas mixture fraction had a significant effect on the code predictions, but the fluctuations in the inlet gas mixture fraction had negligible effect.

In the second set of calculations, the primary and secondary differed in composition. A fuel-rich (gasification) case was investigated. In this case, the primary gas consisted of a mixture of 24 weight percent steam and 76 percent argon, while the secondary consisted of 67 percent oxygen and 33 percent nitrogen. The temperatures of both streams were identical (367 K). Predicted gas temperature is shown in Figures III.A-2 and III.A-3. The two-dimensional contour plots in Figure III.A-2 show the general effect of ignoring all turbulent fluctuations on gas temperature. When fluctuations are ignored, the temperature peaks are much higher and the gradients much steeper. Steeper gradients and higher temperature peaks would be expected to significantly impact the calculated gas-phase composition and rate of particle burnout. Figure III.A-3 shows the individual effects of fluctuations in the mixture fractions on centerline gas temperature. It is interesting to note that ignoring both fluctuations simultaneously produced little error in the early region of the reactor, while ignoring only the η fluctuations produced little error in the aft region of the reactor. However, it appears from these calculations that fluctuations in all mixture fractions generally need to be taken into account in order to predict the temperature profile accurately throughout the entire reactor.

Component 1.b -- Code Sensitivity to Thermal Parameters Affecting Devolatilization

To better understand the role of devolatilization in comprehensive modeling, an investigation of the sensitivity of the devolatilization process to several thermal parameters in the code was conducted. Since devolatilization is a thermally sensitive process, it was felt that critical thermal parameters should be identified and refined before incorporating a

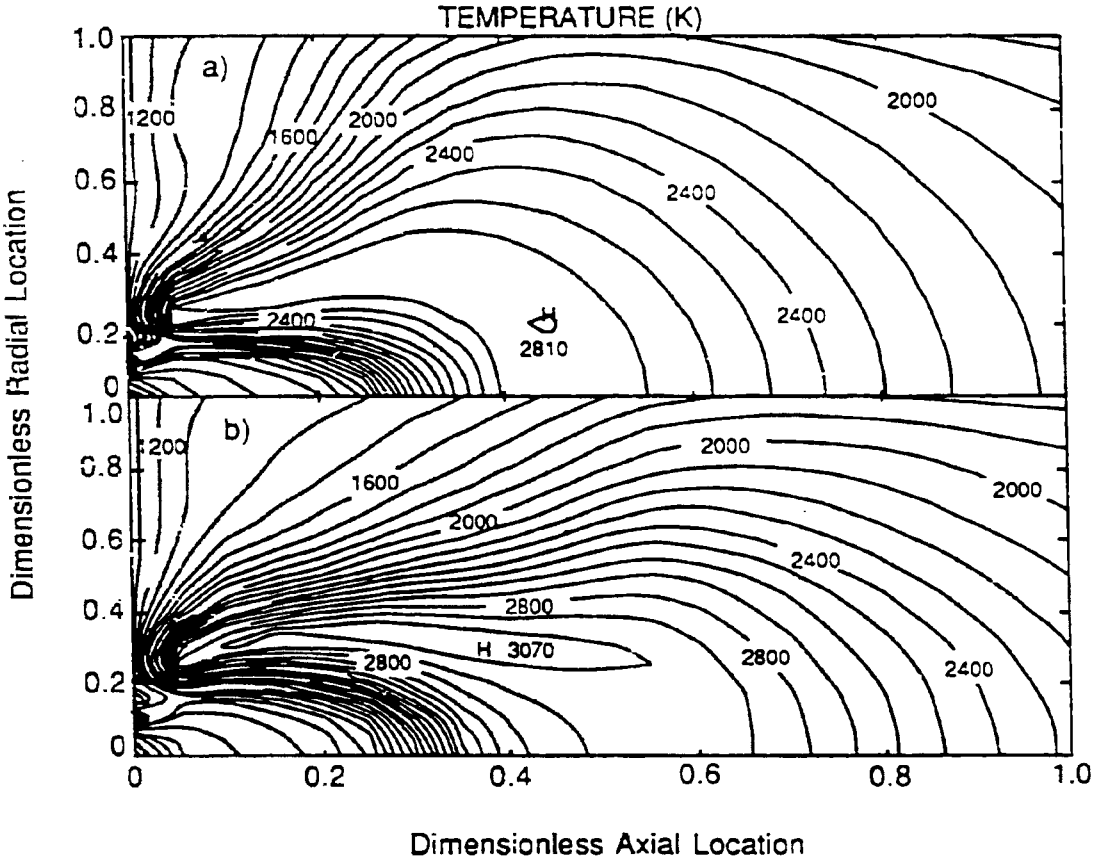

Figure III.A-2. Gas temperature isotherms a) with and b) without fluctuations for case where primary and secondary differ in composition.

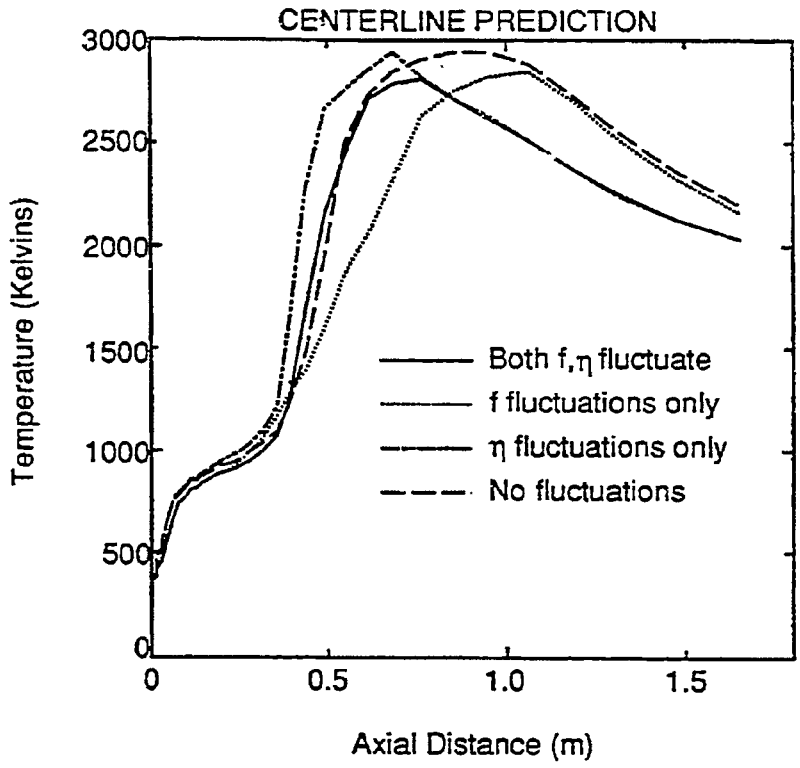

Figure III.A-3. Centerline gas temperature for case where primary and secondary differ in composition.

more detailed model for the devolatilization process. Parameters that were investigated include particle heat capacity, particle emissivity, heat of reaction, and volatiles heating value.

Variable Particle Heat Capacity -- Particle heat capacity was previously modeled in PCGC-2 using quadratic correlations in temperature for coal, char, and ash. Constant values were often assumed, since the temperature dependence of this property was typically unknown. A recent correlation by Merrick (1983) allows heat capacity of coal and char to be calculated as a function of both temperature and composition. The model predicts a maximum specific heat for coal which is nearly twice the room temperature value. Obviously, an accurate model for heat capacity is prerequisite for accurate modeling of devolatilization and the entire coal gasification process.

Merrick's correlation is as follows:

$$c_v = \left(\frac{R}{a}\right)\left[g_1\left(\frac{380}{T}\right) + 2g_1\left(\frac{1800}{T}\right)\right] \qquad \text{(III.A-11)}$$

where g_1 is given by

$$g_1(z) = \frac{e^z}{\left[\frac{(e^z-1)}{z}\right]^2} \qquad \text{(III.A-12)}$$

These equations can be used for both coal and char and predict a monotonic increase in c_v with temperature. However, because composition varies with time, the increase in c_v for a heating and reacting particle may not be monotonic due to changes in average atomic weight (Merrick 1983). The high temperature limit for Eq. III.A-4 is 3R/a, which agrees with established principles of physical chemistry. Using Eq. (III.A-11), Merrick obtained agreement between predicted and experimental values within about 10% over the temperature range of the available data (0-300° C) for various coal ranks (15-35% volatile matter). Graphite and char heat capacities were correlated within 5% over the range 0-800°C.

Calculations carried out under funding separate for single particles of 40 and 100 microns and for a coal-water slurry showed the effect of variable heat capacity on particle temperature and devolatilization rate (Brewster et al., 1987). Calculations performed under this study showed the effect in the comprehensive code. Contour plots (not shown) were similar for the two cases. Temperature was somewhat lower in the variable c_p case due to the increasing value of c_p with temperature and the decrease in volatile yield from the coal. The delay in particle ignition caused by variable c_p was also apparent from these calculations.

The effect of variable heat capacity on total burnout is shown in Figure III.A-4. The curve for variable c_p is shifted to the right, resulting in a decrease of approximately 3 percent in particle burnout at the exit of the reactor. This effect is consistent with the delayed ignition and slightly slower devolatilization rate. Interestingly, the decrease in burnout is approximately equal to the decrease in ultimate volatiles yield predicted for single particles (Brewster et al., 1987), even though particle oxidation was not ignored in the comprehensive code predictions.

Particle Emissivity -- Total emissivities for coal particles have been reported with large variation, as summarized by Solomon et al. (1986). Measurements by Brewster and Kunitomo (1984) for micron-sized particles suggest that previous determinations of the imaginary part of the index of refraction for coal may be too high by an order of magnitude. If so, the calculated coal emissivity for these particles based on previous values may also be too high. The experimental work of Baxter et al. (1987) indicates that the effective emissivity of 100-micron coal particles of several ranks of coal at low temperatures is probably not less than 0.7. Their values are in approximate agreement with those of Solomon et al. (1986).

Calculations were performed to investigate the sensitivity of devolatilization to coal emissivity. Single-particle calculations carried out under separate funding (Brewster et al., 1987) showed little effect for emissivity between 0.9 and 0.1. Comprehensive code calculations for emissivity between 0.9 to 0.3 also showed little effect. The high gas temperature in the single particle calculations made convection/conduction the

principal mode of heat transfer. In the comprehensive code simulations, the secondary air was swirled (swirl no. = 2.0), and the flow field was recirculating. Thus the particles were heated largely by contact with hot recirculating gases and not by radiation. In larger furnaces, or in reactors where the particles do not immediately contact hot gases, radiation may contribute significantly to particle heating, and in this case, greater sensitivity to the value of particle emissivity would be expected.

Heat of Reaction -- Investigators in the literature disagree on both the magnitude and sign of the heat of reaction for coal devolatilization. Reported values range from -65.3 kJ/kg to +334 KJ/kg (Merrick, 1983; Solomon and Serio, 1986). Merrick (1983) speculates that the source of disagreement is related to the effect of variable heat capacity. Heat of reaction probably varies with coal type, however preliminary results (Brewster et al., 1986) indicate that devolatilization calculations are insensitive to this parameter.

Volatiles Heating Value -- Coal volatiles heating value is a function of composition and varies with burnout. However, in comprehensive combustion simulations that treat the effects of chemistry/turbulence interactions, both heating value and composition of the volatiles are often assumed constant. The sensitivity of the comprehensive code to changing volatiles heating value was tested by increasing the heat of formation of the coal. Since volatiles enthalpy was calculated from a particle heat balance with over 80 percent of the total particle mass loss being due to devolatilization, increasing the the heat of formation of the coal effectively increased the volatiles heating value. A value was chosen such that the adiabatic flame temperature of the coal at a stoichiometric ratio of unity was increased by about 200 K. Since the simulations were performed for fuel-lean (combustion) conditions, the actual gas temperatures increased by 50-75 K. The increase was due to both the higher heating value and the increased volatile yield, with the latter effect dominating everywhere except in the near-burner region.

The higher gas temperature significantly affects coal burnout, as shown in Figure III.A-4. with a large portion of the impact coming from the volatile yield in the early regions of the reactor. The magnitude of the variation of

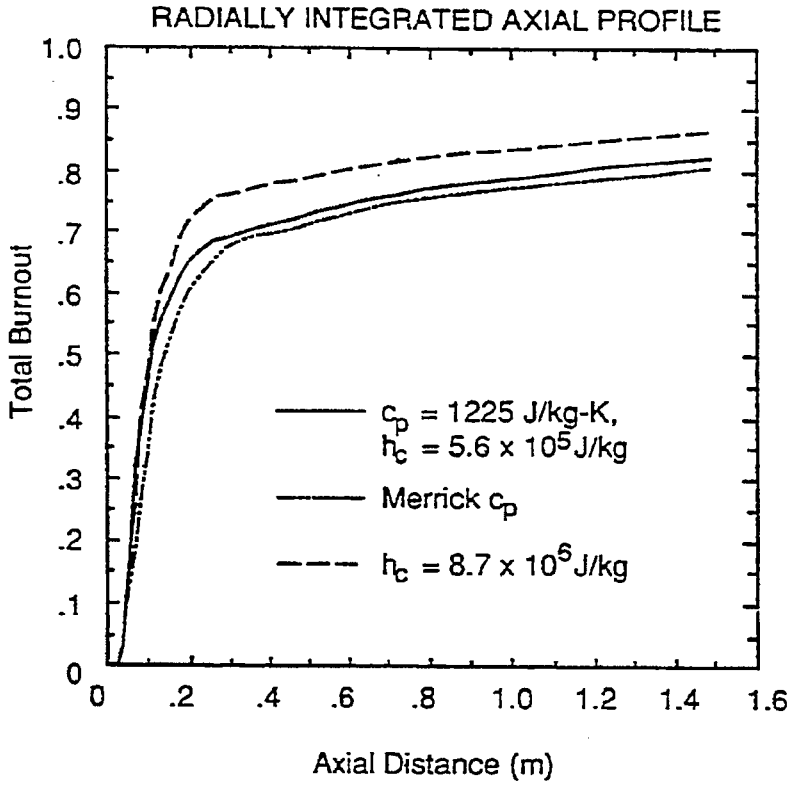

Figure III.A-4. Effect of variable heat capacity and increased volatiles heating value on total particle burnout.

the offgas heating value was arbitrary in this case, but is regarded as representative of actual coals and possibly conservative.

Stastical Gas Dispersion (SGD) Method -- The third method for incorporating the Functional Group Model into PCGC-2 obviates the need for complicated integrations over the mixture fractions by treating the gas phase in a Lagrangian probabilistic fashion to account for the effects of chemistry/turbulence interaction. Baxter (1987) recently developed such a model for the particle phase that distributes the mass source from each particle trajectory throughout the entire reactor, using probability theory, rather than limiting it to the cells through which the particle actually passes. This method offers significant potential for decreasing the required computational time while increasing accuracy and stability, and will be considered under this subtask.

Component 2 -- Incorporating Improved Numerical Solution Methods

The purpose of this component of the subtask is to consider incorporating improved numerical solution techniques that are being developed under separate funding (Smith and Smoot, 1987; Hedman et al., 1987), particularly in this laboratory. No new or improved techniques are being specifically developed under this study. The new methods include improved numerical solvers, distributive relaxation, multigridding, and techniques to take coupling between the equations into account. They hold significant potential for increasing the robustness and speed of the comprehensive code. It is anticipated that these techniques will not be available for incorporation until Phase II of the study; hence, no work was performed on this subtask component during the past year.

Component 3 -- Incorporating SO_x-NO_x Submodel

The aim of this subtask component is to incorporate the SO_x-NO_x submodel being developed under Subtask 2.g into the comprehensive code, and to extend the comprehensive code to include sorbent injection and sorbent chemistry. Work was initiated during the past year on extending the existing pollutant model to include formation of thermal NO and programming this extension into

PCGC-2. This effort is described under Subtask 2.g in this report. The modification to include sorbent injection and chemistry will be based on work being conducted under separate funding at the University of Utah.

Component 4 -- Implementing the Code on Computers

The aim of this component of the subtask is to implement the comprehensive code on several computers, including a workstation. This implementation will require, at a minimum, standardizing the source code so that it will run on a variety of computers. The starting version of the code was developed on a VAX computer with VMS operating system, and VMS Fortran extensions were rampant throughout the code. During the past year, work began to standardize the code to Fortran-77, since the code was partially implemented on the Convex C-1 mini-supercomputer (Berkeley 4.2 Unix operating system). Further standardization is continuing, since the code is currently being implemented on the Sun-3 workstation. Beyond the minimum requirement of Fortran standardization, it is an objective of the program to develop a user-friendly graphics interface. The starting version of the program contained a graphics interface, but that interface cannot generally be implemented on a variety of computers. During the past month, a generic version of the National Center for Atmospheric Research (NCAR) graphics software was obtained for developing such an interface. The NCAR software was selected because it is generally available for a modest cost and because the existing VAX version of the graphics interface for PCGC-2 is based on the VAX version of the NCAR software. Work is underway to implement this software package on the Sun-3 workstation.

Component 5 -- Code Evaluation

The goal of this subtask component is to perform a statistical sensitivity analysis of input parameters to the improved code with advanced submodels and numerical methods incorporated under other components of this subtask. An existing databook will be used as a basis for the evaluation. No work was accomplished specifically under this subtask component during the past year, although the databook is being revised and updated under separate funding (Christensen et al., 1987).

Plans

During the next quarter, work will continue on the three methods of integrating the Functional Group (FG) Model into PCGC-2. The recently developed general devolatilization model (which includes the FG model) will be used to investigate the Single Solids Progress Variable (SSPV) Method where offgas composition and enthalpy are considered constant and the single solids progress variable currently in the code is used to track offgas. Code predictions with the FG Model will be compared to predictions with the two-equation model used previously. Calculations with the two existing progress variables to track volatiles and char oxidation offgas separately will be completed to investigate the Multiple Solids Progress Variable (MSPV) approach. Code predictions with this method will be compared with predictions obtained with the SSPV Method. Consideration will be given to extending the general theory to include correlation between progress variables and incorporating the general theory into PCGC-2. Consideration will also be given to developing the theory of the Statistical Gas Dispersion (SGD) Model, eliminating the need for convolving gas properties over the mixture fractions.

Progress on the development of improved numerical solution methods in this laboratory will continue to be monitored for potential incorporation into the code being developed for this study.

Programming of the extension for thermal NO formation into PCGC-2 will be completed. Progress on the development of a sorbent reaction submodel and its incorporation into a comprehensive code at the University of Utah will continue to be monitored and evaluated for its application to this study.

An updated version of the comprehensive code incorporating the generalized devolatilization submodel and (potentially) an improved particle reaction submodel will be implemented on the Sun 3 workstation. An initial version of the graphics interface will be developed, and the code will be demonstrated and implemented at the Annual Contract Review Meeting to be held at AFR next quarter.

Nomenclature

a	average atomic weight of coal or char (kg/kg-mol)
c_v	constant volume heat capacity (J/kg-K)
g_1	function defined by Eq. (2)
f	gas mixture fraction; inlet gas mixture fraction (dimensionless)
F	transformed mean (dimensionless)
G_f	transformed variance (dimensionless)
g_f	mixture fraction variance (dimensionless)
m	mass (kg)
$\dot{m}$	mass flowrate (kg/s)
$P(f)$	probability density function for mixture fraction (dimensionless)
R	universal gas constant (8314.4 J/kg-mol/K)
T	temperature (K)
z	parameter in Eq. (12)

Greek Symbols:

α	variance (dimensionless)
β	arbitrary gas phase property (various)
η	coal gas mixture fraction (dimensionless)

Superscripts:

$\sim$	Favre-averaged value

Subscripts:

c	coal
h	char
i	i^{th} gas component
i'	i-free gas
p	primary
s	secondary
v	volatiles
0,1,2, ...,N	fluid components defined in mixture fraction approach

III.B. SUBTASK 3.b. - COMPREHENSIVE FIXED-BED MODELING REVIEW, DEVELOPMENT, EVALUATION, AND IMPLEMENTATION

Senior Investigators - Sung-Chul Yi, B. Scott Brewster, and L. Douglas Smoot

Brigham Young University
Provo, Utah 84602
(801) 378-6240 and (801) 378-4326

Objectives

The objectives of this subtask are: 1) to provide a framework for an improved fixed-bed model that can incorporate coal chemistry submodels, improved boundary conditions, and pollutant formation processes; and 2) to provide a basis for evaluating the model.

Accomplishments

Phase I of this subtask has two components: 1) a literature review and evaluation of existing fixed-bed coal gasification models and experimental data, and 2) development of a proposed advanced model. During the first year, a post-doctoral research associate, Dr. Sung- Chul Yi, was hired to work on the project. Accomplishments under each subtask component are described below.

Component 1 -- Literature Review and Evaluation

This subtask component is aimed at 1) reviewing existing models for fixed-bed coal gasification to determine elements that might be used as a starting point for developing the advanced model, and 2) locating experimental data that can be used for model validation. Existing models were reviewed in terms of their level of complexity, method of mathematical solution, extent of validation with experimental data, and availability of a computer code and documentation. Available data are being reviewed in terms of their level of resolution (e.g. in space and time), consistency (e.g. material balance closure), and reliability (e.g. experimental technique used).

Review of Existing Models -- Fixed-bed coal gasification models were recently reviewed by Smoot (1984) and Rinard and Benjamin (1985). These two reviews formed the basis of this review. The review by Rinard and Benjamin (1985) was geared toward finding a model that could be incorporated into the general ASPEN flowsheeting system to compute material balances. Therefore, they were interested in a simple model that could be incorporated into a large flowsheet calculation, with recycle streams, for the express purpose of analyzing the entire flowsheet rather than the detailed design of the gasifier. The purpose of the current project, however, is to develop a model that applies specifically to the fixed-bed reactor. Nonetheless, their review identified the major available models and several characteristics of interest to this study.

The basic approach used in the past has been to view the gasifier in terms of several zones, as illustrated in Figure III.B-1. Coal enters at the top and flows countercurrent to the gas. Air (or oxygen) and other gases such as steam are fed at the bottom. As the coal contacts the hot gases from the bed below, it is progressively dried, devolatilized, gasified, and combusted. The features of several one- and two-dimensional models are summarized in Tables III.B-1 and 2. The fourth column of Table III.B-2 shows potential features of the advanced model to be developed by this study. A brief description of each of the existing models is given below. The proposed elements of an advanced model are discussed later.

University of Delaware (UD) Models -- Both 1-D and 2-D models were developed at the University of Delaware. Both models predict transient effects, and both assume equal solids and gas temperatures. The emphasis of the UD models is on high-pressure, slagging gasification. For the solid-particle-gas reactions, two particle models were used. These are the Ash Segregaton (AS) and Shell Progressive (SP) models. The AS Model assumes the ash detaches from the outside surface of the char particle as soon as it is completely reacted. In this case, the apparent reaction rate is given by (Denn et al., 1982):

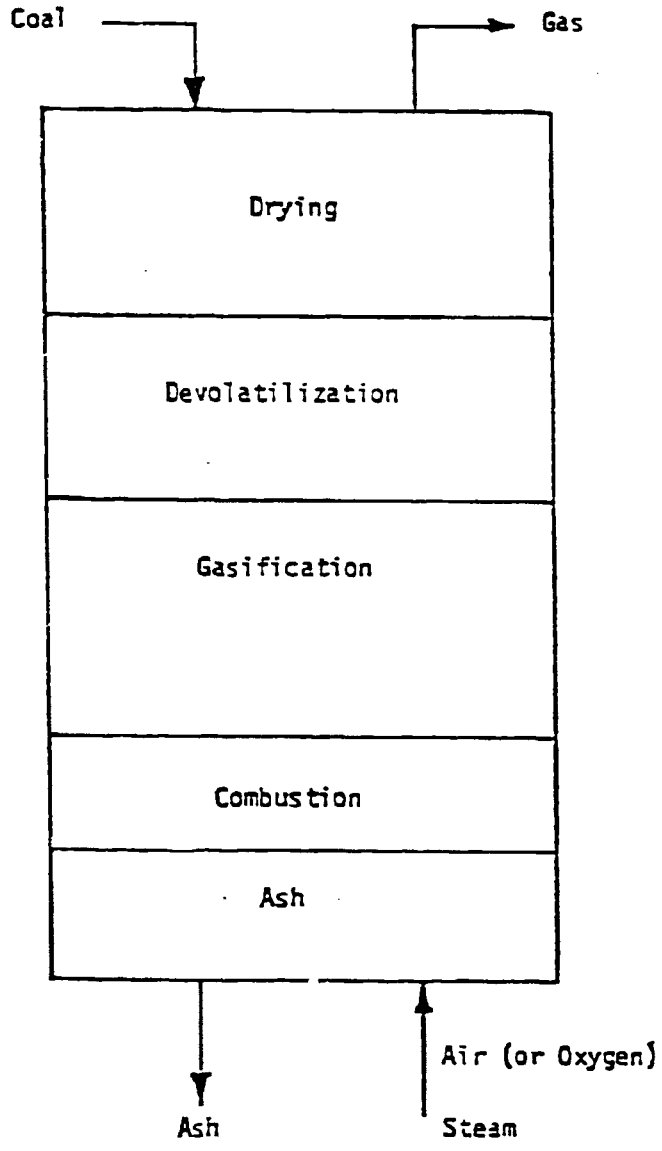

Figure III.B-1. Typical zones in a moving-bed gasifier.

Table III.B-1
Review of selected 1-D fixed-bed Models

Source	Author Year	Scope	Emphasis	Key Assumptions	Species	Code/Manual
Washington University Model	Cho and Joseph/1981 Kim and Joseph/1982	1-D, hetero-geneous, steady, transient.	gasification; moving-bed; countercurrent	plug flow for gases & solid; separate devol. process; with & without H_2 burning reaction; radiation through k_{eff} & h_{eff}.	char + 6 gas species	no manual code avail. from Joseph
University of Delaware Model	Yoon et al. 1977/1978	1-D, homo-geneous, transient, steady,	gasification; moving-bed; countercurrent; high P, slagging	no heat loss to boundary layer; small radiative effect; equil. water-gas rxn; amount of coal devol. equal amount of volatile matter specified in proximate analysis; all the gasification rxns are reversible	char + 6 gas species	code/manual avail. from EPRI
West Virginia University Model	Hon et al. 1982	1-D, homo-geneous, steady.	gasification; moving-bed; countercurrent	kinetic parameters for various coal types; no drying zone; radiative & convective heat-transfer; plug flow for gases and solid; coal particle model for devol.	char + 6 gas species	code/manual avail. from METC
ASPEN/ RGAS Model	Rinard & Benjamin 1985	1-D, homo-geneous, steady.	gasification; moving-bed; countercurrent	kinetic models from WVU Model and UD Model; devolatilization is totally empirical; small radiative effect.	char + 6 gas species	code/manual avail. from DOE

Table III.B-2
Comparison of Candidate 2-D Fixed-Bed Models

	University of Delaware Model	Lawrence Livermore Laboratory Model	Washington Univ. Model	Potential Advanced Model Features
Author Year	Denn et al. 1982	Thorsness & Kang 1986	Bhattacharya et al. 1986	Current Study
Scope	homogeneous, moving-bed, steady/transient	homogeneous, packed-bed, transient	homogeneous, fixed-bed, transient	heterogeneous, fixed-bed, moving-bed, steady/transient
Radiation	through k_{eff} & h_{eff}	through k_{eff}	through k_{eff} & h_{eff}	diffusion approximation method
Coal reaction	AS[1] model	AS & SP[2] model	SP model	AS, SP, & general coal rxn model
Species	char + 6 gas species	2 solids + 7 gas species	char + 6 gas species	general gas species (gas rxn. equil., solids kinetics)
Devolatil-ization/ Pyrolysis	instantaneous heating,thermally neutral	not included	separate devol. process	general devol./ pyrolysis submodel
NO_x,SO_x Submodel	not included	not included	not included	can include
Evaluation	overall performance of 1-D & 2-D Model for Lurgi		bench-scale gasifier data	existing data (limited); sensitivity analysis
Mineral behavior	not included	not included	not included	will consider
Application	gasification, gasification/combustion	underground coal	gasification	
	combustion high pressure, slagging	gasification	moving-bed	various fuels mild gasification,
CPU time		CDC 7600 2845 s for 41 nodes	1.5 hrs on DEC-20	
Numerical efficiency		vectorization		
Code/Manual	code/manual avail. from EPRI	no manual,code avail. from Kang	no manual,code avail. from Joseph	code/manual will prepare

$$r_i = \frac{(1-\varepsilon)(P_i - P_i^*)V_c}{\frac{d_p^o \rho}{6k_{pi}} + \frac{1}{\eta_i k_{ri} C_c^o}} \qquad \text{(III.B-1)}$$

The SP Model, on the other hand, assumes the ash remains on the surface, and the oxidizer diffuses through the ash layer to get to the unreacted core where it reacts. In this case, the apparent reaction rate is given by (Denn et al., 1982):

$$r_i = \frac{(1-\varepsilon)(P_i - P_i^*)}{\frac{d_p^o}{6k_{pi}} + \frac{d_p^{o\,2}(1-\rho)RT}{12\rho D_{Mi}} + \frac{1}{\eta_i \rho^3 k_{ri} C_c^o}} \qquad \text{(III.B-2)}$$

The definitions of the above variables are listed in the Nomenclature at the conclusion of this section of the report. The AS and SP models represent two extremes of ash behavior. The behavior of coal particles in dry-ash gasifiers and combustors probably lies somewhere between these two extremes. For slagging gasifiers, however, the molten ash probably drips off the particles, resulting in behavior that is closer to the AS Model. The effects of particle size distribution were ignored in the UD models.

Plug flow was assumed for the gases in the 2-D model. Radiation was accounted for by using an effective heat transfer coefficient and thermal conductivity. Computer codes and user manuals for both models are available from the Electric Power Research Institute (Denn et al., 1982).

Washington University (WU) Models -- Both 1-D and 2-D models were also developed at Washington University. As with the UD models, both WU models predict transient effects. The 1-D model allows for separate gas and solids temperatures, but the 2-D model assumes equal gas and solids temperatures. Both models assume plug flow for the gas and solid phases, and devolatilization is segregated from the rest of the coal reaction process. The SP model was used to describe the apparent rates of reaction. Radiation is taken into account through effective values for thermal conductivity and heat transfer coefficient. Computer codes for both models are available

from Babu Joseph at Washington University. User manuals are not available, however.

West Virginia University (WVU) Model -- This 1-D model is steady-state and assumes equal gas and solids temperatures. A computer tape and user manual (Wen et al., 1982) are available from METC. The manual contains kinetic parameters for various types of coal, as well as sample problems and comparisons with experimental data. The manual also illustrates how to use the code to prepare maps of reactor operation to aid in design. A unique feature of the WVU model is its ability to predict tar formation.

ASPEN/RGAS Model -- This 1-D model was developed for the ASPEN flowsheeting system. Its purpose is to predict gasifier effluent properties to aid in material balance calculations in flowsheet design and optimization. The model can readily incorporate any desired kinetics. The computer code and kinetics packages corresponding to the WVU and UD models are available as a part of the ASPEN system, and use of the model has been documented by Rinard and Benjamin (1985). Devolatilization is empirical, with the user supplying a list of volatile products and their yields.

Lawrence Livermore Laboratory (LLL) Model -- This 2-D model was developed to model underground coal gasification. The model assumes equal gas and solids temperatures, and predicts transient effects. Radiation is included through effective thermal conductivity, and Darcy's law is used to predict the gas velocity profile. A computer program is available, but there is no user manual.

Other Models -- Amundson and Arri (1978) developed a rigorous mathematical model for the reaction taking place around a single char particle. The model was used in studying the gasification of char in a countercurrent reactor.

Stillman (1979) developed a 1-D, heterogeneous moving-bed gasifier model. Char gasification, combustion, devolatilization, and drying were all

described by kinetic equations. He did not include the burning of hydrogen to water in his kinetic model.

Evaluation of Computer Codes -- Computer codes for the UD and WU 2-D models were obtained and installed on the VAX-11/780 computer at BYU. In addition, a code for the LLL model was obtained and installed on the Convex/C-1 computer. After installing the UD and WU codes, sample problems were executed and compared with published results. After correcting a minor error in the calculation of the orthogonal matrix in the WU code, sample problem results were successfully reproduced. The correction had only a minor effect on the code predictions. Attempts to reproduce sample problem results for the UD code have been unsuccessful. These efforts have been complicated by the fact that the sample problem input data provided in the documentation are incompatible with the version of the program that was supplied.

The LLL code was developed on a Cray computer and requires extensive changes to run it on another computer. To aid in making the conversion, the computer center at Lawrence Livermore Laboratory prepared a tape containing a partial conversion of the program to standard Fortran. The remaining changes and installation at BYU have not been completed, however.

This effort to implement and operate available 2-D fixed-bed codes has provided useful insight into these codes. Assessment of generality, user friendliness, user's manual structure, and numerical solution methods has contributed substantially to formulation of an advanced fixed-bed model. While none of the available codes has been identified as an appropriate framework for the advanced model, efforts to operate these codes for comparative purposes will continue.

Review of Experimental Data -- A search was initiated to identify data for model validation. Space- and time-resolved data are of particular interest. Unfortunately, such data are scarce, at least in the public sector. However, several sets of effluent data and partial space-resolved data have been identified. Gas flow data without reaction in fixed-beds are

also being sought to validate model predictions for the fluid mechanics of fixed beds.

The experimental data of five bituminous coals, one subbituminous coal, and one lignite coal from the METC gasifier have been obtained (Desai and Wen, 1978; Wen et al. ,1982; Stefano, 1985). These data include dry product gas distribution, exit gas temperature, and percent carbon conversion, for several operating conditions (coal, steam, and air feedrates; and pressure). Similar data have been obtained for the Lurgi gasifier, the British Gas Corporation (BGC) gasifier and the General Electric (GE) gasifier (Stefano, 1985). A bench-scale, 4-inch-diameter, fixed-bed gasifier was designed and built by Salam (1983) at Washington University. Two experimental runs were carried out using Wyoming Wyodak char. In these experiments, transient temperature profiles at five axial positions and two radial positions were measured. Transient product gas compositions were also measured.

A rather extensive set of data was obtained from the Wellman-Galusha gasifier at the Twin Cities Research Center (Minneapolis, Minnesota) of the U.S. Bureau of Mines (Thimsen et al., 1985). As shown in Table III.B-3, data were obtained for seventeen different types of coal (bituminous, subbituminous, and lignite), peat, and coke. Material balances and thermal efficiency calculations over several selected periods during each test are available. The output items in the mass/energy balance are gasifier operation data, coal data, tar and water yield (dry basis), ash and dust data (dry basis), and gas composition (dry basis). Some profile data for temperature and pressure are also reported.

METC gasifier data reported by Stefano (1985) and Wen et al. (1982) for various coals will be used to evaluate the model for the effects of coal type, boundary conditions, and mode of operation. The Wellman-Galusha gasifier data reported by Thimsen et al. (1985) will also be used. Bed temperature profiles reported by Salam (1983) and Eapen (1979) in a bench-scale reactor will also be used.

Table III.B-3

Solids Fuels Used in Fixed-Bed Gasification Tests Conducted at Black, Sivalls & Bryson Inc. (Thimsen et al., 1985)

Bituminous

Jetson Bituminous
Stahlman Stoker
Piney Tipple Bituminous
River King Bituminous
Elkhorn Bituminous
Blind Canyon Bituminous
Hiawatha Bituminous
SUFCO Bituminous

Subbituminous

Rosebud Subbituminous
Leucite Hills Subbituminous
Absaloka Subbituminous
Kemmerer Subbituminous

Lignite

Benton Lignite
Indianhead Lignite

Peat

Peat Pellets
Peat Sods

Coke

Delayed Pet. Coke

Component 2 - Detailed Plan for Fixed-Bed Model

General Features -- The purpose of this component of the subtask is to develop an advanced fixed-bed model. The model may be based on an existing model or combination of models, or it may be developed from scratch, whichever seems more appropriate. From the literature review and evaluation of existing codes under Component 1, the desired characteristics and requirements of an advanced fixed-bed model were sought. A research plan for developing the advanced code will be formulated under Subtask 1.b and presented to METC during the next quarter.

Characteristics and Requirements -- Based on the review of models and data, potential elements of an advanced fixed-bed model have been identified. Several of these elements were summarized in Table III.B-2. Due to the presence of radial temperature and (presumably) concentration gradients, the advanced code should be 2-dimensional. Devolatilization and other solids reaction processes should be generalized, using the large particle submodel being developed under Subtask 2.e. Due to the finite rate of heat transfer between the solids and gas, and the importance of predicting solids temperature accurately for the detailed particle submodel, gas and solids temperatures should vary independently. Extension of the gas-phase reactions to include a wider variety of species, can be considered, assuming thermodynamic equilibrium. Frozen equilibrium on chemical kinetics may be required for liquid products important in mild gasification. Formation and destruction of pollutant species can also be considered, based on the submodel of the entrained-bed code (Subtask 2.g). Solids flow is a particularly critical issue in fixed-bed modeling. Assumption of plug flow is considered to be inadequate. Relating irregular solids flow to coal conversion (Thorsness and Kang, 1986) is viewed as a reasonable starting point. Based on this set of general features, the formulation of the proposed advanced model is outlined below. This information provides a basis for expert consultant evaluation and for presentation to METC.

Energy and Material Balance Equations -- All of the existing 2-D models listed in Table III.B-2 assume identical gas and solids temperatures. Stillman (1979) showed with his 1-D model that substantial temperature differences may exist between the phases. Figures III.B-2 and 3 show his calculations for a dry-ash and a slagging gasifier. The temperature profiles in both figures are very similar in shape but differ by hundreds of degrees. These temperature differences are larger in the slagging than in the dry ash gasifier. Predicting solids temperature is likely to be important to predicting the onset of slagging, and will also be important to the detailed particle reaction kinetics submodel.

Figure III.B-4 shows radial temperature profiles at various axial positions from the bottom of the gasifier calculated by Denn et al. (1982) using their 2-D model. Substantial temperature gradients are indicated near the wall. This result was also observed by Bhattacharya et al. (1986) in small-scale, fixed-bed gasifier tests. The results obtained at BYU with the WU model are shown in Figure III.B-5. The profiles in Figure III.B-4 are flat in the center because the UD model assumes an adiabatic central core.

The 2-D steady-state energy balance equations for the gas and solid streams extended from Stillman's 1-D formulation (1979) are:

Gas stream

$$\frac{1}{r}\frac{\partial}{\partial r}\left(rk_{rg}\frac{\partial T_g}{\partial r}\right)+\frac{\partial}{\partial z}\left(k_{zg}\frac{\partial T_g}{\partial z}\right)-v_{rg}\sum\rho_{g,i}C_{pg,i}\frac{\partial T_g}{\partial r}-v_{zg}\sum\rho_{g,i}C_{pg,i}\frac{\partial T_g}{\partial z}$$

$$+h_{gs}a_{gs}(T_s-T_g)+\sum(-\Delta H_k)r_k=0 \qquad \text{(III.B-3)}$$

Solid stream

$$\frac{1}{r}\frac{\partial}{\partial r}\left(rk_{rs}\frac{\partial T_s}{\partial r}\right)+\frac{\partial}{\partial z}\left(k_{zs}\frac{\partial T_s}{\partial z}\right)-v_{rs}\sum\rho_{s,i}C_{ps,i}\frac{\partial T_s}{\partial r}-v_{zs}\sum\rho_{s,i}C_{ps,i}\frac{\partial T_s}{\partial z}$$

$$-h_{gs}a_{gs}(T_s-T_g)+\sum(-\Delta H_j)r_j=0 \qquad \text{(III.B-4)}$$

The wall temperature distribution may be assumed one-dimensional, and is given by (Bhattacharya,1985)

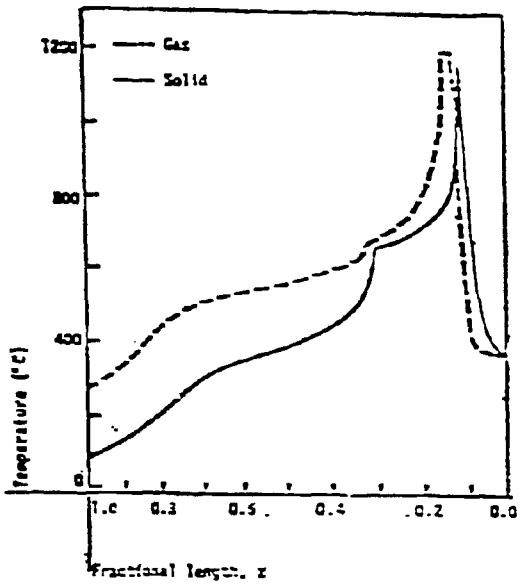

Figure III.B-2. Temperature profiles in ash reactor (figure taken from Stillman, 1979).

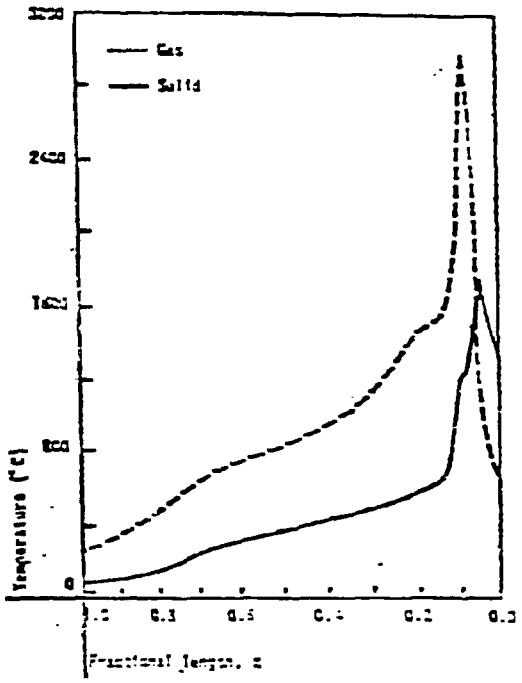

Figure III.B-3. Temperature profiles in slagging reactor (figure taken from Stillman, 1979).

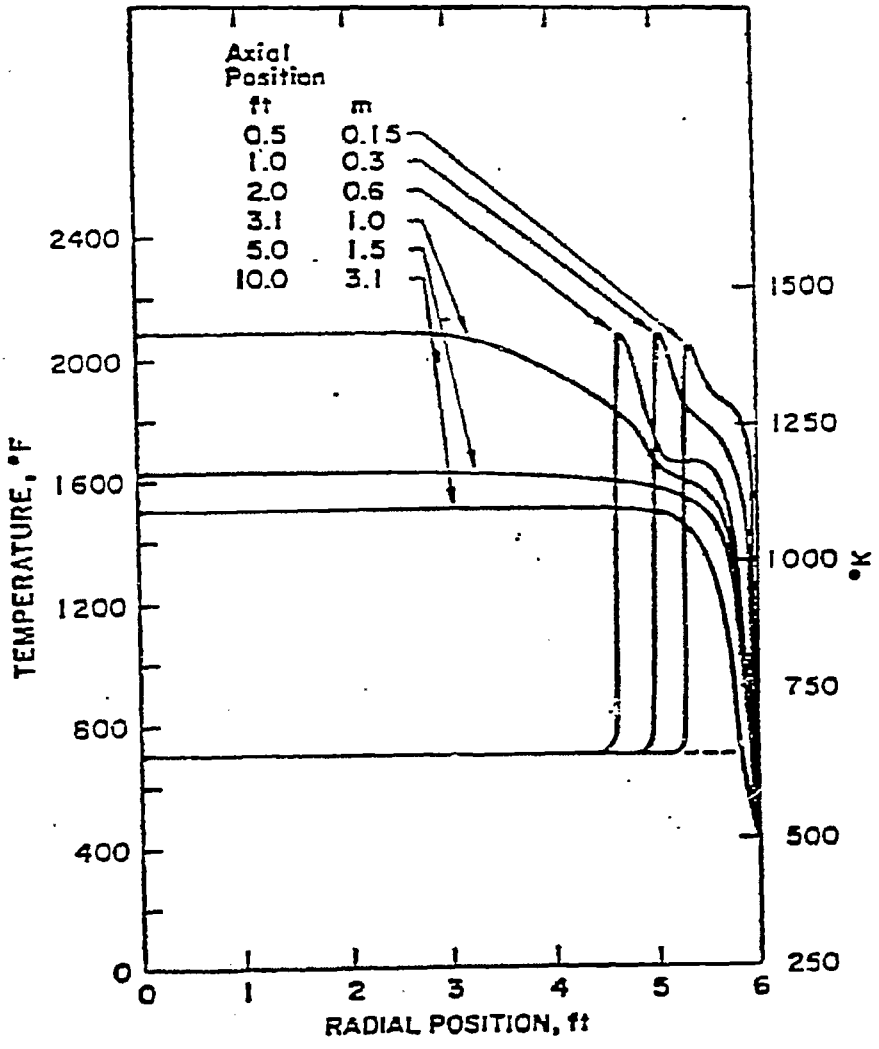

Figure III.B-4. Radial distribution of temperature at various axial positions of UD model (figure taken from Denn et al., 1982).

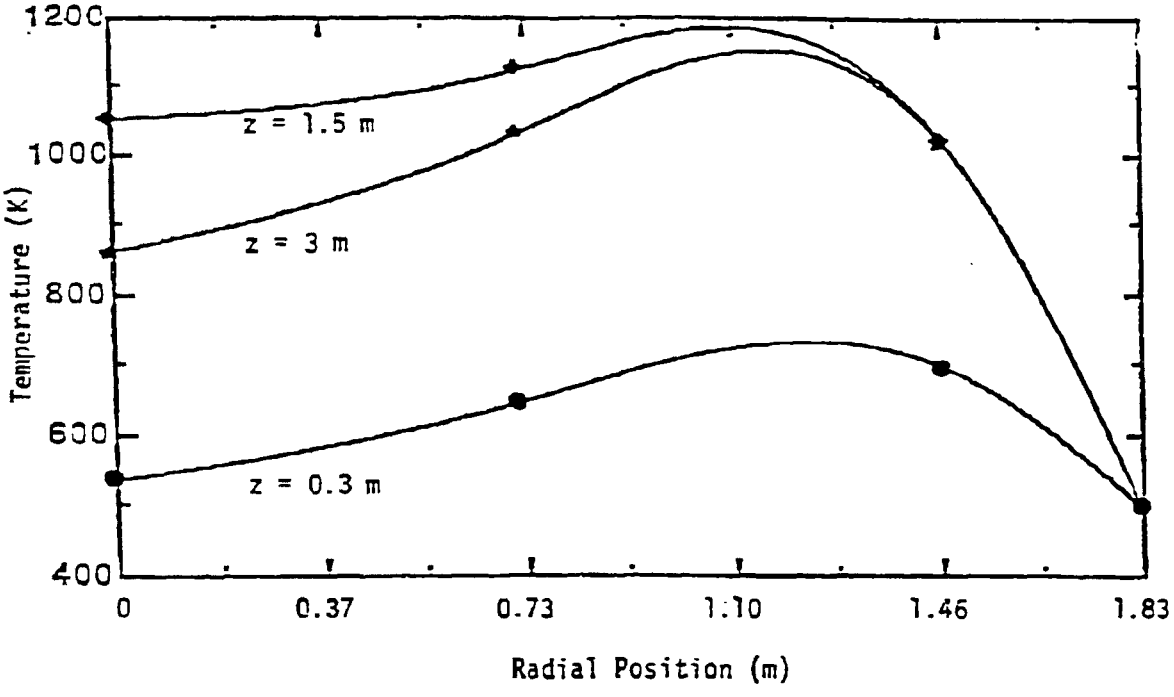

Figure III.B-5. Radial distribution of temperature at various axial positions of WU model (calculated in our laboratory).

$$2Rh_{eff}(T_{g_{r=R}} - T_w) + 2R_o h_o(T_\infty - T_w) + k_w(R_o^2 - R^2)\frac{\partial^2 T_w}{\partial z^2} = 0 \qquad \text{(III.B-5)}$$

The gas-phase material balance of species i can be written as (Denn et al. (1982):

$$\frac{1}{r}\frac{\partial}{\partial r}(rD_{rg,i}\frac{\partial C_{g,i}}{\partial r}) + \frac{\partial}{\partial z}(D_{zg,i}\frac{\partial C_{g,i}}{\partial z}) - v_{rg}\frac{\partial C_{g,i}}{\partial r} - v_{zg}\frac{\partial C_{g,i}}{\partial z} - \sum \alpha_{ik} r_k = 0 \qquad \text{(III.B-6)}$$

The solid-phase species material balance is (Thorsness and Kang, 1986):

$$\frac{1}{r}\frac{\partial}{\partial r}(rD_{rs,i}\frac{\partial C_{s,i}}{\partial r}) + \frac{\partial}{\partial z}(D_{zs,i}\frac{\partial C_{s,i}}{\partial z}) - v_{rs}\frac{\partial C_{s,i}}{\partial r} - v_{zs}\frac{\partial C_{s,i}}{\partial z} - \sum \beta_{ij} r_j = 0 \qquad \text{(III.B-7)}$$

The boundary conditions are:

$$z = 0 \quad C_{g,i} = C^o_{g,i} \quad T_g = T^o_g \quad \frac{\partial T_w}{\partial z} = 0 \qquad \text{(III.B-8)}$$

$$z = L \quad C_{s,i} = C^o_{s,i} \quad T_s = T^o_s \quad \frac{\partial T_w}{\partial z} = 0 \qquad \text{(III.B-9)}$$

$$r = 0 \quad \frac{\partial T_s}{\partial r} = 0 \quad \frac{\partial T_g}{\partial r} = 0 \quad \frac{\partial C_{g,i}}{\partial r} = 0 \quad \frac{\partial C_{s,i}}{\partial r} = 0 \qquad \text{(III.B-10)}$$

$$r = R \quad k_{rg}\frac{\partial T_g}{\partial r} = h_{eff}(T_{g_{r=R}} - T_w) \quad k_{rs}\frac{\partial T_s}{\partial r} = h_{eff}(T_{s_{r=R}} - T_w)$$
$$\frac{\partial C_{g,i}}{\partial r} = 0 \quad \frac{\partial C_{s,i}}{\partial r} = 0 \qquad \text{(III.B-11)}$$

Work is needed to determine which terms in Eqs. (III.B-3 through 11) should be included in the solution. For example, there is some evidence that radial and axial heat dispersion should be included, but that corresponding mass dispersion terms might be neglected. The effect of axial and radial dispersion of heat and mass can be examined by the

simulation results of the UD model (Denn et al., 1982). Table III.B-4 shows the Reynolds number and Peclet numbers for heat and mass transfer in the axial and radial directions at various carbon loadings. In general, a Peclet number is defined by

$$Pe = \frac{\text{characteristic velocity} * \text{characteristic length}}{\text{characteristic dispersion}} \qquad \text{(III.B-12)}$$

Axial and radial mass dispersions are relatively unaffected by carbon loading. However, the thermal Peclet numbers become so small at one percent carbon load that thermal dispersion is important. Further, it has been suggested that inclusion of transient accumulation terms may aid in the numerical solution, while also providing a more general code.

Gas Fluid Mechanics -- The one-dimensional momentum equation for a packed bed of porous media is given by (Ergun, 1952):

$$-\frac{\varepsilon^3}{(1-\varepsilon)}\frac{d_p}{\rho_g u_g^2}\frac{dP_e}{dz} = 150\frac{(1-\varepsilon)\mu}{d_p\rho_g u_g} + 1.75 \qquad \text{(III.B-13)}$$

$$P_e = P + \rho_g gz \qquad \text{(III.B-14)}$$

The first term on the right side of Eq. (III.B-13) is the viscous term, which is negligible if the bed Reynolds number (Re) is greater than 1000, and the second term, the inertial force, is negligible for Re less than 10; here Re is defined as (Denn et al., 1982)

$$Re = \frac{d_p\rho_g v_s}{(1-\varepsilon)\mu} \qquad \text{(III.B-15)}$$

Figure III.B-6 (Ergun, 1952) shows pressure-drop data for flow through porous media. The Lurgi moving-bed gasifier operating at full load has a Reynolds number of approximately 200, in the transition region where both force terms are important according to the above figure. A momentum balance in the radial direction is required to establish a two-dimensional gas flow

Table III.B-4
The Reynolds Number, the Axial and Radial Mass Transfer and Thermal Peclet Numbers at various Carbon Loadings of the Lurgi Gasifier.

% of Carbon Load	Re	$Pe_{m,a}$	Pe_m	$Pe_{h,a}$	$Pe_{h,r}$
100	200	2	10	0.6	4.6
50	100	2	10	0.6	3.5
10	20	3	10	0.5	1.0
1	2	3	7	0.1	0.1

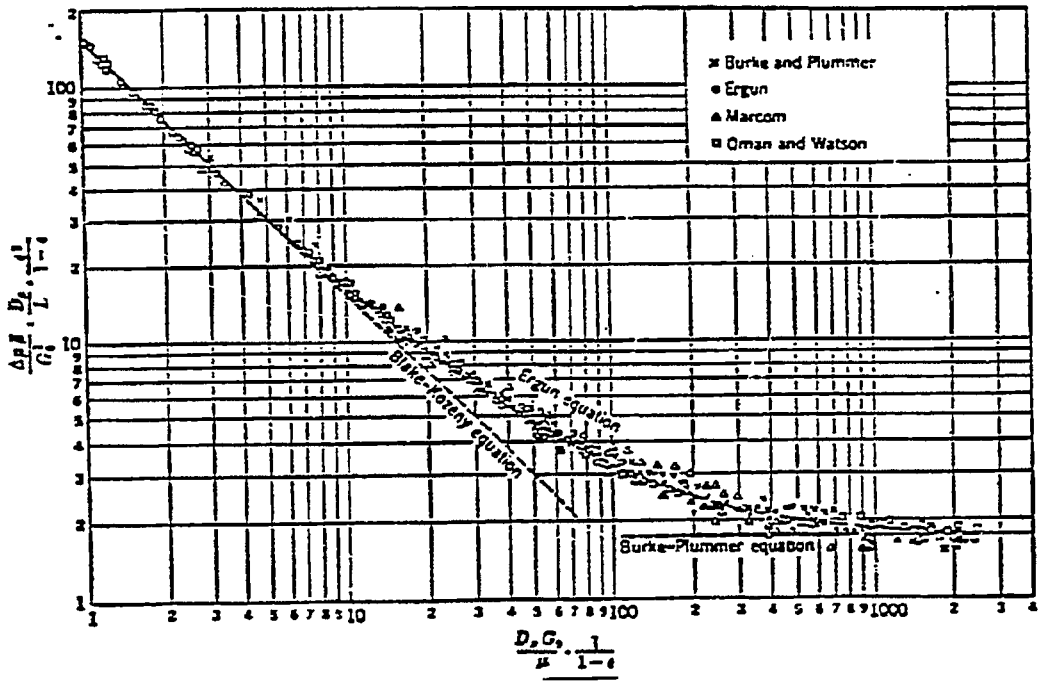

Figure III.B-6. The pressure-drop data for flow through porous media (taken from Ergun 1952).

pattern. If it is assumed to have the same form as Eq. (III.B-13), the momentum equation can be written as

$$-\frac{\varepsilon^3}{(1-\varepsilon)}\frac{d_p}{\rho_g v_g^2}\nabla P_e = 150\frac{(1-\varepsilon)\mu}{d_p\rho_g v_g} + 1.75 \qquad \text{(III.B-16)}$$

When this equation is substituted in Eqs. (III.B-3 and 6), the gas velocities can be eliminated.

The void fraction and particle size distribution are important in determining gas flow in a moving-bed gasifier. If both are assumed to vary with carbon conversion, then

$$\varepsilon = f(\varepsilon_o, X_c) \qquad \text{(III.B-17)}$$

$$d_p = f(d_p^o, \varepsilon_o, X_c) \qquad \text{(III.B-18)}$$

Solids Flow -- In order to solve the energy/mass balances of the solid phase, a bed-settling model (Thorsness and Kang, 1986) will be considered for the solid velocity. Overall bed density will be assumed constant with no dispersion of the solids as they move straight downward. Then the solids velocity can be written as

$$v_s = v_{so} + \frac{1}{\rho_s}\int_0^z g\,dz \qquad \text{(III.B-19)}$$

where v_{so} denotes the solid particle velocity at the bottom of the bed and the z coordinate is the bulk-flow or vertical direction.

Solids Kinetics Models -- The Functional Group (FG) devolatilization model predicts the chemical species that are evolved and the rates at which they are evolved. Inclusion of this submodel in the advanced fixed-bed code is planned. Large particles will not heat rapidly or uniformly, so a single temperature cannot be used to characterize the entire particle. The internal char surface provides sites where secondary reactions can occur. Devolatilization products generated near the center of particle must migrate to the outside to escape. During this migration, they may crack, condense,

or polymerize, with some carbon deposition taking place. The process of large particle devolatilization depends upon both chemical kinetics and internal mass and heat transfer. Many of these issues are being considered for large particles in Subtasks 2.e and 2.f. The large particle submodel being developed under Subtask 2.e will provide the basis of solids reaction modeling in the comprehensive code.

Amundson and Arri (1978) did not include a devolatilization submodel in their model for single char particles. However, their gasification model seems to have significant potential for considering devolatilization simultaneously with other particle reactions. They postulated a shell-progressive mechanism determined primarily by the reaction

$$C + 1/2\ O_2 \rightarrow CO \qquad \text{(III.B-20)}$$

at the core surface, while in the core of the particle the gasification of carbon with CO_2 and steam together with the water-gas-shift reaction takes place. Very fast reactions between gasification products (CO and H_2) and O_2 are assumed, and the existence of a flame front either at the core surface or in the ash layer is possible. From outside such a flame front, the whole process can be visualized as the simple reaction

$$C + O_2 \rightarrow CO_2 \qquad \text{(III.B-21)}$$

with the outer region under simple O_2-CO_2 equimolar countercurrent diffusion. If the O_2 concentration in the bulk phase is too low (or the core temperature too high), the flame front will not occur at the core surface as it might at higher O_2 concentrations, but will detach from the core surface. In the latter case, all of the O_2 will be exhausted either in the ash layer, if one has been formed, or in the boundary layer by reaction with H_2 and CO produced in the core of the particle.

In order to solve Eqs. (III.B-3 through 7), expressions are needed for the production rates, characterizing solid-gas interactions. For this purpose, the particle models described in the UD model (Denn et al., 1982), such as the AS model and SP model, as well as a general volume reaction

model can be used. For the AS and SP models, a single particle size (monodisperse) is treated (Denn et al., 1982); however, extension to a more general case of various initial size distributions is possible (Thorsness and Kang, 1986).

Four heterogeneous reactions are the most prominent in the gasification and combustion zones. These are:

Gasification zone

$$Char + H_2O \text{ --------> } CO + H_2 \qquad \text{(III.B-22)}$$

$$Char + CO_2 \text{ --------> } 2CO \qquad \text{(III.B-23)}$$

$$Char + 2H_2 \text{ --------> } CH_4 \qquad \text{(III.B-24)}$$

Combustion Zone

$$xChar + O_2 \text{ --------> } Ash + 2(x-1)CO + (2-x)CO_2 \qquad \text{(III.B-25)}$$

Gas Reactions Model -- Existing models include a limited number of gas phase reactions. However, a promising approach assumes gas-phase equilibrium or partial equilibrium and computes the gas phase composition using a general-purpose algorithm such as CREK (Combustion Reaction Equilibrium Kinetics)(Smoot and Smith, 1984). This approach allows practical prediction of many more species in the gas phase than the kinetics approach using global reactions. Radicals such as OH and O can be included as well as pollutant species such as NH_3, HCN, SO_2, and H_2S. Of course, some gas-phase kinetics may need to be taken into account, such as for nitrogen pollutant reactions.

Liquid Products -- The FG/DVC model provides an excellent basis for extending the range of model applicability to include mild gasification, where the gasifier is operated at moderate temperatures in order to enhance the production of liquids. These species are producerd near the top of the bed during devolatilization and must be treated by a non-equilibrium approach, such as partial equilibrium or frozen flow.

Radiation -- Amundson and Arri (1978) studied the effect of radiation in fixed beds by means an apparent axial thermal conductivity. Figure

III.B-7 shows a comparison between steady-state profiles with and without radiation for the case of a dry-ash reactor. In this figure, it can be seen that there is a dramatic lowering of the peak temperature when radiation is considered. Most models include radiation using an effective thermal conductivity. This method is described by Vortmeyer (1978). However, the diffusion approximation method (Brewster, 1987) may be applicable to fixed-bed coal gasification due to the optical thickness of the bed material. The diffusion approximation solution of the general radiative heat transfer equation for an absorbing/emitting/scattering medium, in a heavily loaded system with a small mean-free-path of photons relative to the system dimensions is (Brewster, 1987):

$$q_r = (-\frac{4}{3})(\frac{\sigma}{K_a + K_s})\nabla T^4 \qquad \text{(III.B-26)}$$

When linearized about T_0, the expression becomes:

$$q_r = (-\frac{16}{3})(\frac{\sigma T_o^3}{K_a + K_s})\nabla T \qquad \text{(III.B-27)}$$

$$K_a + K_s = \frac{1.5\, f_v Q_e}{d_p} \qquad \text{(III.B-28)}$$

where Q_e is the extinction coefficient, which is approximately unity. The radiation effect can be incorporated by simply substituting the above equation into an solid energy balance equation. Near the wall, the diffusion approximation may not be valid due to the small values of optical thickness. This difficulty may be overcome by using a jump boundary condition technique discussed by Ozisik (1972).

Pollutant Formation -- A pollutant submodel will be considered, based on the submodel being extended and developed for the entrained-bed code under Subtask 2.g. SO_x species can be obtained directly from a generalized local equilibrium solution. NO_x will likely require kinetic treatment.

Solution Methods -- Denn et al.(1982) used orthogonal collocation on finite elements for the radial coordinate, and integrated the resulting

ODE's by a fourth order Runge-Kutta method. For the dynamic case, he used exponential collocation in the time domain. Bhattacharya et al.(1986) also used collocation for the radial dimension and finite differencing in the time dimension, so that the set of PDE's could be rewritten as a large set of ODE's in the axial direction. This set of equations was numerically integrated using Gear's routine (1971), which utilizes a predictor and backward-differencing corrector.

The use of orthogonal collocation was popularized by Villadsen and Stewart (1967). In this method, the approximate solution of a differential equation is expressed as a combination of orthogonal polynomials. The zeros of the selected orthogonal polynomials are the collocation points. Furthermore, the solution of the ODE can be expressed in terms of the values of the dependent variable at the collocation points instead of the values of the coefficients of the trial functions. Numerical comparisons of orthogonal collocation to various finite difference methods (Michael and Iordache, 1976) and finite element methods (Hopkins and Wait, 1978) have been published. Collocation has been found to be superior to the Runge-Kutta fourth order method for boundary value problems and some initial value problems containing steep gradients (Villadsen and Sorensen, 1969) in speed of calculation and stability.

Thorsness and Kang (1986) used the method of lines (MOL) to solve the partial differential equations described in their model. The MOL solution scheme is based on the solution of a set of initial-value ordinary differential equations. These ODE's are obtained from the PDE boundary value problem of interest by discretizing the PDE's in the spatial dimensions. This yields a set of ODE's with time as the independent variable. A suitable ODE solver is then used to integrate the system of equations in time to yield the required results. The power of the method stems primarily from choosing one of the very powerful ODE solvers currently available. The ODE solver must be able to handle the stiff system which results from the discretization of the spatial dimensions and from the physics of the problem. It should also provide a straightforward method of time-step and error control. Thorsness and Kang (1986) used LSODE, a widely

available software package developed at Lawrence Livermore Laboratory by Hindmarsh (1980).

In independent work at the BYU Combustion Laboratory, evaluation and implementation of advanced numerical methods has been a major thrust. Methods include multiple gridding, equation coupling, vectorizing, and efficient solver techniques. Once the fixed-bed model is formulated, a review of alternative solution methods will be considered.

Recommendation and Key Issues -- The fixed-bed review has provided the basis for development of an improved fixed-bed gasification/combustion model. It is recommended that an improved fixed-bed model be developed. Generalizing coal reaction processes, treatment of pollutants and radiation, and improved treatment of solids and gaseous flow processes are the principal areas for focus. Sensitivity analysis of model parameters and evaluation of the fixed-bed model through data comparisons also constitute significant areas for emphasis, as do numerical methods. Even though data for model comparisons are limited, newer data provide an improved base for comparison. This recommendation and the proposed fixed-bed model will be reviewed by consultants before the recommendation is presented to METC.

Fixed-bed combustors and gasifiers are very complex, and the state of model development is only in its initial phases. There are significant gaps in fundamental processes that are not well characterized. The development and thorough evaluation of the proposed improved model can be an important advance. Yet, it must be recognized that this effort will not resolve all of the uncertainty associated with fixed-bed modeling. Some of the issues that are not currently adequately resolved include the following:

1. Solids Flow. Available treatment of solids in plug flow is not adequate. Solids vary in particle size initially, and continue to change through conversion in the bed.

2. Gaseous Flow. Permeabilities in porous beds of changing material are uncertain. Application of velocity-pressure drop correlations for non-reacting packed beds in reacting, two-dimensional flows is

uncertain. The treatment of the injector/distributor region adds complexity. There may be some straight-forward basic measurements such as coal and ash permeability that will give insights into the model components.

3. Limited Experimental Data. Recent data provide an expanded base for model evaluation. However, the data are still limited. Little data on gas concentration profiles are available. No data on separate gas and particle temperatures are reported, and apparently, no pollutant profile data are available. Effluent data from fixed-beds are not an adequate test of model value.

4. Behavior of Ash. Ash adds several complexities to fixed-bed behavior. The ash may form around the particle, inhibiting the char conversion and altering heat transfer. Small ash particles change the gas and solids flow behavior. Agglomeration and slagging complicate solids transport.

5. Particle Reaction Processes. Use of a wide distribution of large coal feed particle sizes, temperature gradients within large particles, ash behavior, and differences in particle and gas temperature complicate this complex set of processes. Requirements to generalize the coal devolatilization submodel (and the char oxidation submodel) add to this complexity.

6. Gas Equilibrium Solution. Gas equilibrium is a reasonable approach that may not be more uncertain than global kinetics and has some generalized advantages, where detailed gas composition, including some pollutants, is predicted. Treatment of partial equilibrium or frozen flow in segmented regions or for specific species may be useful.

7. Liquid Products. Gas equilibrium is likely to break down for fuel-rich species at low temperatures, such as in mild gasification. Treatment of partial equilibrium or frozen flow in segmented regions or for specific species may be useful.

8. Numerical Solution Methods. Although steady-state solutions are of major interest, a transient model would be more general and would allow for calculation of steady-state solutions as well. In addition, the transient model may be more stable and robust since the steady-state solution is obtained by evolving through physically real states. In addition, some of the data available for model validation are unsteady-state. Because of the disparity of gradients that exist in the bed, adaptive gridding should be used, particularly in the z-direction.

9. Unjustified Complexity vs. Generality. It is desirable to formulate a model with sufficient generality to test the inclusion of questionable terms in the equations and to be applicable to a wide range of conditions. However, model generality leads to additional complexity requiring greater computational resources and, therefore, needs to be justified.

Plans

Plans for the next quarter include completion of the evaluation of the WU and LLL models. A review meeting will be held with expert consultants to evaluate the proposed advanced model. The technical literature survey of submodels will be continued. A databook containing important datasets for model evaluation will be initiated. Recommendations will be made to METC for fixed-bed model development.

Nomenclature

a_{gs}	Particle surface area per unit bed volume [1/m]
$C_{g,i}$	Gas concentration of species i [mol/m3]
C_i	Concentration of gas species i [mol/m3]
$C_{ps,i}$	Heat capacity of solid species i [J/mol-k]
$C_{pg,i}$	Heat capacity of gas species i [J/mol-k]
C^o_c	Initial concentration of fixed carbon in the coal particle [mol/m^3]
$D_{ea,i}$	Axial effective mass dispersion of gas species i [m^2/s]
$D_{ea,c}$	Axial effective mass dispersion of solid [m^2/s]
$D_{er,c}$	Radial effective mass dispersion of solid [m^2/s]
$D_{ea,i}$	Radial effective mass dispersion of gas species i [m^2/s]
$D_{M,i}$	Effective diffusivity of gaseous i in the ash shell [m_2/s]
d_p	Particle diameter [m]
d^o_p	Initial particle diameter [m]
f_v	Particle volume fraction [-]
g	Solid carbon productions per unit volume of bed [kg/m3 s]
h_{gs}	Film heat transfer coefficient [J/m2 hr K]
h_{eff}	Effective wall heat transfer coefficient [J/m2 hr K]
h_o	Wall surrounding heat transfer coefficient [J/m2 hr K]
K_a	Absorption coefficient [-]
K_s	Scattering coefficient [-]
k_{as}	Axial conductivity of solid phase [J/m s K]
k_{rs}	Radial conductivity of solid phase [J/m s K]
k_{ag}	Axial conductivity of gas phase [J/m s K]
k_{rg}	Radial conductivity of gas phase [J/m s K]
$k_{r,i}$	Intrinsic reaction rate constant of reaction i [-]
k_{pi}	Mass transfer coefficient of gaseous species i through bulk film
k_s	Effective conductivity of inside the particle [J/m s K]
Pe	Hydrostatic pressure [Pa]
P	Static pressure [Pa]
P_i	Partial pressure of gaseous species i [Pa]
P^*_i	Equilibrium partial pressure of gaseous species i [Pa]
Q_e	Extinction coefficient [-]
R	Gas constant [J/mol K]

r	Radial distance [m]
r_i	Reaction rate [mol/m^3 s]
T	Temperature [K]
T_c	Surrounding temperature [K]
T_g	Gas phase temperature [K]
T_s	Solid phase temperature [K]
T_w	Wall temperature [K]
T_0	Ambient temperature [K]
T_∞	Surrounding temperature [K]
v_{ag}	Axial superficial gas velocity [m/s]
v_{rg}	Radial superficial gas velocity [m/s]
v_{as}	Axial superficial solid velocity [m/s]
v_{rg}	Radial superficial solid velocity [m/s]
v_{so}	Superficial solid velocity at the bottom of the bed [m/s]
V_c	Fraction of original solid volume occupied by unreacted fixed carbon (Ash Segregation Model).
X_c	Fraction of fixed carbon remaining in the coal [-]
z	Axial distance [m]

Greek:

α_{ij}	Stoichiometric coefficient [-]
β_{ij}	Stoichiometric coefficient [-]
ε	Porosity [-]
ε_0	Initial porosity [-]
ρ	Ratio of the size of unreacted core to initial particle size
ρ_g	Gas density [kg/m^3]
μ	Average gas viscosity [Pa s]
η_i	Effectiveness factor of reaction i
σ	Stefan Boltzman Constant [J/s m^2 K^4]